Time dependent Stokes shifts of fluorescent dyes in the hydrophobic backbone region of a phospholipid bilayer: Combination of fluorescence spectroscopy and ab initio calculations

Jan Sýkora[1,*], *Petr Slavíček*[2,1], *Pavel Jungwirth*[3], *Martin Hof*[1]

[1] J. Heyrovský Institute of Physical Chemistry, Academy of Sciences of the Czech Republic, Dolejškova 3, 18223, Prague 8, Czech Republic

[2] Department of Physical Chemistry, Prague Institute of Chemical Technology, Technická 5, Prague 6, 166 28, Czech Republic

[3] Institute of Organic Chemistry and Biochemistry, Academy of Sciences of the Czech Republic, and Center for Biomolecules and Complex Molecular Systems, Flemingovo nám. 2, Prague 6, 16610, Czech Republic

KEYWORDS: anthroyloxy-dyes, solvation dynamics, molecular dynamics, fluorescence spectroscopy, ab initio calculations.

[*]Corresponding author: jan.sykora@jh-inst.cas.cz

ABSTRACT

We explored the time dependent Stokes shifts of fluorescent dyes containing an anthroyloxy-chromophore (2-AS, 9-AS, and 16-AP) in bilayers composed of dimyristoyl-phosphatidylcholine (DMPC). The obtained data revealed a non-trivial solvation response of these dyes, which are located in the backbone region of the bilayer with a gradually increasing depth. For comparison, steady state emission spectra in the neat solvents of various polarity and viscosity were also recorded. The results indicate that on the short picosecond time scale the AS-dyes undergo complex photophysics including formation of states with a charge transfer character. This observation is supported by ab initio calculations of the excited states of 9-methylanthroate. The slower nanosecond part of the relaxation process can be attributed to the solvation response of the dyes. A slowdown in solvent relaxation is observed upon moving towards the center of the bilayer. A mechanism similar to preferential solvation present in the mixture of a polar and non-polar solvent is considered to explain the obtained data.

1. **Introduction**

Hydration of biological molecules and self-assemblies enables their proper functioning and enhances their stability. Water molecules present in the hydration layer are proved to have completely different intermolecular structure and dynamical properties compared to the bulk solution. For instance, solvation dynamics is slowed down remarkably.[1] Phospholipid bilayers, which form a basic part of cellular membranes, belong to the most important biological systems. With respect to their structure we distinguish three main regions, each with unique features: the interface, the headgroup, and the backbone region. The interface region includes the surface bilayer and the interacting water molecules. Here, solvation dynamics takes place on a rather broad time-scale (with reported picosecond, subnanosecond up to nanosecond components).[2,3] The intrinsic fluctuations in the bilayer, and the spread of chromophore locations leads to a broad distribution of different microenvironments and thus, to the observed "unspecific" solvent relaxation (SR) dynamics. The headgroup region consists of fully hydrated functional phospholipid groups. The solvation dynamics is slower than at the interface region and is reported to occur exclusively on the nanosecond time-scale.[3] The rather complex structure of the hydrated and charged headgroup region, however, makes the application of molecular dynamic (MD) simulation for explaining the observed nanosecond kinetics rather difficult.[4]

The backbone region is composed of the hydrophobic chains of fatty acids where the water content was found to be low.[5] The only fluorescent dyes suitable for monitoring the solvation dynamics in this region are presently the probes with the anthroyloxy-ring attached to the fatty acid chain at various positions (known as n-AS dyes) (Figure 1). These probes were reported to be located at a well-defined graded series of depths along the normal axis of the bilayer.[6,7] It is known for a long time that anthroyloxy-based dyes can serve as sensitive polarity probes.[8-11] It is, therefore, possible to use n-AS for investigating the water concentration profile in the backbone region. The aim of this paper is to demonstrate the usefulness of n-AS dyes also for probing the dynamics of water in the backbone region.

An important insight into the nature of solvation dynamics can be provided by MD simulations. These were applied for studies of, e.g. chromophores dissolved in a polar solvent[12] or at the liquid/liquid

interfaces,[13] chromophores located in a mixture of polar and non-polar solvents[14] or in polar nanoclusters.[15] The latter two cases are specifically important for the discussion of solvation dynamics in the backbone region of the bilayer. In both cases the chromophore is incompletely solvated by the polar solvent. MD studies lead to identifications of different solvation timescales connected with different molecular motions: starting from a femtosecond timescale for the librational solvent response, over a picosecond timescale for solvent rearrangements around the chromophore up to the nanosecond diffusion component corresponding to the flow of the solvent molecules towards/from the excited chromophore.

The goal of this work is to probe solvation dynamics by recording the time resolved emission spectra (TRES) in varying depths of the backbone region of the bilayer. Large unilamellar vesicles (LUVs) composed of dimyristoyl-phosphatidylcholine (DMPC) lipid molecules are used as a model system. The inspection of TRES is supposed to bring new insights into the properties and structure of the water molecules present in the labeled regions. However, the TRES spectra contain information not only about the solvation dynamics but potentially also about intramolecular processes. In case of AS dyes, the photophysics is rather complex and still not fully understood. It has, e.g., never been fully satisfactorily explained why fluorescence behavior of anthroyloxy-based dyes is strongly solvent dependent. Detailed understanding of the intramolecular dynamics of the respective dyes is, however, vital for a correct interpretation of the TRES spectra. To this end, the present experiments on 2-AS, 9-AS, and 16-anthroyloxy-palmitoic acid (16-AP) are also accompanied by data collected at various temperatures in different solvents of varying polarity and viscosity. The aim is to obtain a more thorough understanding of the photophysics of these dyes which enables interpretation of the results gained from TRES.

In addition, the photophysics of the dyes is rationalized by means of quantum mechanical calculations on a smaller model system of 9-methylanthroate. Results of theoretical calculations allow us to understand the time dependent fluorescence behavior of anthroyloxy-dyes, assigning different processes to individual time scales.

The paper is organized as follows. In section 2, the employed experimental and theoretical methods are described. Results together with a discussion are presented in the third section. Section 4 concludes the paper with an outlook for future studies.

2. Materials and methods

2.1 Experimental methods

All probes, (2-(9-anthroyloxy)stearic acid (2-AS), 9-(9-anthroyloxy)stearic acid (9-AS) and 16-(9-anthroyloxy)palmitic acid (16-AP)), see Figure 1, were purchased from Molecular probes and were used without any further purification. Phospholipids (dimyristoylphosphatidylcholine (DMPC) and dipalmitoylphosphatidylcholine (DPPC)) were supplied from Avanti Lipids. All solvents of spectroscopic grade were purchased from Merck. The preparation of DPPC and DMPC large unilamellar vesicles (LUVs) was performed as described previously extruding with 100 nm filters.[16] Absorption spectra were recorded on a Perkin-Elmer Lambda 19 spectrometer. Fluorescence spectra and decays were recorded on a Fluorolog 3 steady state spectrometer (Jobin Yvon) and on an IBH 5000 U SPC equipment. Low temperature steady state spectra were measured on a modified Edinburgh Instruments FLFS900 spectrometer. Decay kinetics was recorded using a Picoquant PLS-370 excitation source (370 nm peak wavelength, 500 ps pulse width, 5 MHz repetition rate) and a cooled Hamamatsu R3809U-50 microchannel plate photomultiplier. The primary data consisted of a set of emission decays recorded at a series of wavelength spanning the steady-state emission spectrum. The time-resolved emission spectra (TRES) were gained by the spectral reconstruction method.[17] Full width at half maxima (FWHM) and emission maxima ($\nu(t)$) profiles of the reconstructed TRES were obtained by a log-normal fitting.[17] The correlation functions $C(t)$ were calculated according to:

$$C(t) = \frac{\nu(t) - \nu(\infty)}{\nu(0) - \nu(\infty)} \qquad (1)$$

where $\upsilon(0)$ and $\upsilon(\infty)$ correspond to the value obtained by "time 0 estimation" and to the value at time infinity, respectively. The obtained $C(t)$ were fitted with a sum of exponentials as described in Horng et al.[17]

$$C(t) = \sum_{i}^{3} a_i \exp(-t/\tau_i) \quad (2)$$

where a_i and τ_i correspond to the amplitude and characteristic time, respectively.

Finally, the kinetics of the solvation dynamics was parametrized with the so called relaxation times τ_r:

$$\tau_r = \int_0^{\infty} C(t)dt \quad (3)$$

Generally, in the studies investigating solvation dynamics the solvent relaxation time τ_{SR}, which is defined as an integral of the correlation function, describes the kinetics of SR quantitatively. We define above the integral relaxation time τ_r which is an analogy to the SR time. However, it characterizes the time course of the overall relaxation process including both the internal intramolecular relaxation and solvent relaxation.

2.2 Computational methods

We have performed electronic structure calculations in order to investigate possible photochemical mechanisms. Several levels of description have been employed. For entry level calculations the semiempirical AM1 Hamiltonian has been utilized. To deal with excited states, the FOMO-CAS(6/6) scheme has been used.[18] Since the semiempirical parametrization is not adequate to describe potential energy surface far from the equilibrium geometries, we have used ab initio techniques to address this issue. Ground state minimum of the investigated dye (9-methylanthroate) has been obtained at the MP2/6-31g* level. For exploration of the potential energy surfaces of the excited states, we have used the CAS-SCF method with an active space consisting of 6 electrons in 6 orbitals with the same basis set as above. At this level we have also performed excited state geometry optimization. At the optimized geometries we have performed single point CASPT2 calculations. During the CASPT2 calculations, 40 orbitals have been kept frozen to make the calculation numerically feasible. The results are, however, not particularly sensitive to the exact number of orbitals kept frozen. The calculations are essentially stable with respect to change of the active size and the number of states over which we average the energy during the orbital optimization.

All the CAS-SCF and CASPT2 calculations have been performed with the MOLPRO electronic code package.[19] The semiempirical calculations have been performed with the modified version of the MOPAC package.[20]

3. Results and Discussion

In this section we discuss first the photophysics of the AS-dyes on the basis of the absorption and steady-state fluorescence spectra. Consequently, interpretation of the spectra is then deduced from *ab initio* calculations. Second, we investigate the TRES measured in the backbone region of the phospholipid bilayer. Solvation and intramolecular dynamics of AS-dyes in biomembranes is then discussed in the context of the present findings about their photophysics.

3.1 Absorption and excitation spectra in different environments

Absorption and excitation spectra were measured for the set of n-(9-AS) (n = 2, 9) and 16-(9-AP) dyes in a wide range of solvents, and in DMPC and DPPC large unilamellar vesicles. All recorded spectra show features characteristic for anthracene with three well-distinguished peaks corresponding to the 0-2, 0-1, and 0-0 transitions (the numbers stand for the vibrational levels in the ground and excited states, respectively).[21] The obtained values for the three main peaks of the excitation and absorption spectra are identical for all measured systems within the experimental error of 50 cm^{-1}. Maxima of excitation spectra of 2-AS are summarized in Table 1 for selected solvents and lipid systems. Only a small shift of a maximal value of 200 cm^{-1} is detected for a large range of solvents and vesicle systems. Table 2 shows the values of the middle peak maxima of the excitation spectra for the set of n-(9-AS) (n = 2, 9) and 16-(9-AP). Again, the excitation spectra and the absorption spectra (not shown here) appear to be largely invariant within the whole set of these compounds. In summary, the absorption and excitation spectra depend neither on the chromophore environment nor on the position of attachment of the fatty acid chain.

3.2 Fluorescence emission spectra

In contrast to the absorption and excitation spectra, both shape and position of the emission steady state spectra show significant differences when modifying the polarity and viscosity of the solvent.

In non-polar solvents, on one hand, there are at least two fluorescence bands apparent in the steady state spectra indicating contributions from at least two energetically different fluorescent states (see figure 2A). Moreover, with the increase of viscosity the peak corresponding to the more energetic state becomes more pronounced, as is obvious for the data recorded in paraffin oil (figure 2B). On the other hand, in polar solvents, the steady-state spectra loose their fine structure and particular bands are no more recognizable. In addition, the spectra are broadened and red shifted in contrast to the non-polar solvents. Both in the case of polar and non-polar environments, the recorded fluorescence spectra do not bear the mirror image relation to the absorption spectra. Apart from the dependence of the fluorescence spectra on the polarity and viscosity, an effect of the position of the anthroyloxy group can be observed.

In DMPC vesicles the steady state spectra of 2-AS and 9-AS are rather similar to those observed in polar solvents. In addition, they show the expected trend and the deeper location of the dye leads to a slight blue shift of the emission spectrum possibly due to the polarity gradient within the bilayer (figure 3B). In contrast, the character of the fluorescence spectrum for 16-AP is similar to that observed in a non-polar environment. Moreover, it is red-shifted in comparison to the steady state spectra recorded for 2-AS and 9-AS. This fact may be explained by inspecting time resolved emission spectra (see section 3.5). Bearing in mind that the observed steady state spectrum is actually a sum of the time resolved emission spectra and that the 16-AP shows the fastest relaxation process of all three dyes (section 3.5), it is obvious that the more relaxed (i.e., more red-shifted) states contribute to the steady state spectrum more markedly than in case of 2-AS and 9-AS dyes.

3.3 Quantum chemical calculations and the discussion of the n-AS photophysics

In order to gain further insight into the photophysics of the n-AS dyes, we have explored the excited state potential energy surface of 9-methylanhroate (9MA) by means of quantum chemical methods. The

9MA molecule (see Figure 1B) is lacking the long alkyl chain and carboxylic group of the n-AS molecules but it has the same anthracene based chromophore, capped with a methyl group. It is, therefore, an excellent model system for this type of compounds. The emission spectra of n-AS dyes and their dependence on the solvent polarity, viscosity and temperature are qualitatively identical to those of 9MA.

Experimental information for this molecule is available both for different solvents and for an isolated molecule in the gas phase. 9MA molecule has been studied experimentally in condensed phase[8,22,23] and in supersonic jets.[24] Semiempirical calculations have been also performed on this molecule.[10]

The absorption spectra of this molecule exhibit anthracene like structure with a negligible solvent shift. This is in accord with the fact that both the ground and excited state dipole moments are rather low. The fluorescence spectra of 9MA are, on the other hand, strongly red-shifted and diffuse. The Stokes shift is highly solvent dependent. The dipole moment change estimated from Lippert-Mataga equation provides a value of 4.5 D.[8] The fluorescence spectra do not bear the mirror-image relation with the absorption spectra for any solvent. The above features are also true for the 9MA molecule in the gas phase. Any suggested photochemical scheme of the 9MA dye has to explain those features, as well as the polarity, temperature and viscosity dependence of the n-AS fluorescence spectra.

The absence of the mirror image relation of the fluorescence and absorption spectra in the non-polar solvents and even in the gas phase clearly indicates that a significant intramolecular relaxation takes place upon the photoexcitation, which also holds true for AS-dyes embedded in the membrane.[25] Two possible mechanisms can be considered: (1) Conformational relaxation along the twisting coordinate, or (2) formation of different structures, some of them of a charge-transfer character.

The first mechanism has been suggested by Swayanbunathan and Lim[24] for the 9MA molecule and further used by Berberan-Santos and coworkers[9] to rationalize the photophysics of the 12-AS molecule. According to this explanation, the absorption occurs mainly from the twisted configuration that is not preferential for the excited state. As a result, the excited chromophore starts to relax by intramolecular rotation. The increasing viscosity of the environment slows down the intramolecular rotation and leads

to emission from initial or partially relaxed states resulting in the growth of the blue shifted shoulder of the steady state spectrum. There are, however, some difficulties with this idea. By looking at the steady state spectra in heptane and in viscous paraffin oil (figure 2A, 2B) of all n-AS dyes and by inspecting the temperature scan of 2-AS in heptane from 300 K to 150 K (figure 4A) we can safely distinguish at least two emitting states. It is unclear how such a feature could be produced by an emission from a single well. The intramolecular relaxation should also be in this case much faster than that observed in the time resolved fluorescence experiments. Neither does the rotational relaxation mechanism explain why such a modest rearrangement could destroy the mirror image character of the fluorescence spectrum. As a matter of fact, the fluorescence spectrum of analogical methylester of the 9-acridencarboxylic acid in tetrahydrofuran does not exhibit the broad, red-shifted spectrum of 9MA even though the torsional potential both in S_0 and S_1 states and their absorption spectra are very similar.[26]

Further evidence against the rotational relaxation mechanism comes from the present electronic structure calculations. The first excited state in the Franck-Condon region is essentially the anthracene ring $\pi\pi^*$ state. This is a non-polar state, with a dipole moment being within 1D from its ground state value. The torsional curves calculated with a semiempirical AM1 Hamiltonian for the S_0 and S_1 states are depicted in Figure 5. The twisting angle in the ground state is 60^o, in the S_1 relaxed state it is 50^o (CAS-SCF optimization provides similar numbers of 58^o and 53.5^o for the two states). The barrier at 90^o in the S_0 state is less than 0.02 eV, thus it is thermally accessible, the barrier in the S1 state being also low (0.04 eV). This is in a good agreement with previous calculations of Dey[26] for a free acid and the height of the barrier also agrees with the experimental estimate of Swayanbunathan.[24] The Stokes shift between the Franck-Condon point and the relaxed locally excited state minimum is less than 0.3 eV. These semiempirical calculations are also in a semi-quantitative agreement with CAS-SCF and CASPT2 calculations (Table 3). The dipole moment does not change significantly along the rotational coordinate. Neither the value of the Stokes shift nor the solvent dependence is, therefore, in agreement with the rotational relaxation mechanism.

We thus addressed a question whether there is a different geometry on the S_1 potential energy surface which would be energetically accessible, possibly lower in energy than the locally excited state. Such a structure should be of a charge transfer character (and should, therefore, have a large dipole moment) to explain the observed polarity dependence. The search for these local minima has been performed using the CAS-SCF method with the results are summarized in a Table 3 and in Figure 6. The potential energy surface of the 9MA molecule in its first excited state is rather complex. We may anticipate that for different atomic configurations the S_1 state will be dominated by configurations with a $\pi\pi^*$ transition localized in the ring, $\pi\pi^*$ transition within the COOMe moiety, $n\pi^*$ transition or the charge transfer $\pi\pi^*$ transition. We have localized several distinct minima on the S_1 potential energy surface with energy bellow or comparable with that of the locally excited (LE) state (see Figure 6). These minima are denoted as Min1, Min2, and Min3. Min1 corresponds to a S_1 state minimum with a large dipole moment (6.5 Debye). This fits nicely with the estimate of a 9MA dipole moment change by Werner.[8] Also the estimated emission wavelength from this structure, 470 nm at the CASPT2 level, and large transition dipole moment for the emission from this state support the idea that we observe this structure in the fluorescence emission spectra. Note also that the CT state found here is further stabilized in polar solvents. Geometrically, this structure has a bent anthracene ring with a ring carbon atom connected to the out of plane carbonyl group. The anthracene ring in this structure is bent by some 25^o. There is a single bond between the carboxylic carbon and the anthracene group while the C=O bond remains a double one. The O=C-C_{anthr}-C dihedral angle is close to zero, however the carboxyl group is not coplanar with the anthracene ring because of its distorsion. We have also found a structure originally suggested by Werner with a double bond between the anthracene ring and the carboxyl part (Min2). This state is, however, dominated by an excitation within the carboxylic group. The anthracene ring is bent in a similar way as found for a Min1 structure. We have also localized a third minimum on the S_1 potential with a planar ring geometry, elongated C=O bond, and pyramidilized carboxylic carbon (Figure 6). The two latter structures are energetically close to the LE state. However, the transition dipole moment is much smaller than that of Min1. Also the dipole moments of these structures are

rather similar in S_0 and S_1 states. This does not exclude the possibility that they contribute to the fluorescence spectra; structure of this type can be the source of the second peak observed in the experiment. Note that these states are energetically close to higher states with much larger transition dipole moments. The fact that the emission spectrum does not possess the mirror relation with the absorption spectrum even in non-polar solvents suggests that the above states or at least some of them (presumably the state of the C=O $\pi\pi^*$ character) might be responsible for the second, more energetic peak in non-polar solvents.

We can, therefore, conclude that the following mechanism is likely to take place:

S0 → S_1 (FC) → LE → CT state

LE → other distorted emitting states

While the motion towards the locally excited minimum is essentially barrierless, the opposite is true for the second process. The intramolecular relaxation can thus take much longer times than was originally expected. We discuss this issue in section 3.5. Note that the conical intersection between S_2 and S_1 states (found from the locally excited minimum) has a geometry somewhere in-between the locally excited minimum and structure Min1. This intersection is energetically close to the locally excited state, suggesting that there will be only a small barrier for the escape from the locally excited state.

3.4. Temperature scans

In order to validate the conclusions drawn from the theoretical simulations, we have performed temperature scans in heptane (figure 4A) and in an ethanol-methanol mixture (figure 4B). With decreasing temperature both polarity and viscosity are increasing. This interplay leads to a non-monotonous dependence of the solvent shift on the temperature. With the ethanol:methanol mixture we can reach a glassy state which completely freezes most of the short time conformational dynamics.

In the case of ethanol:methanol mixture the temperature decrease from 300 K to 200 K leads to a gradual red-shift of the fluorescence, probably due to the increase of solvent polarity and consequent higher stabilization of the states possessing a charge transfer character. In addition, solvent relaxation is likely to contribute to the red-shift since at these temperatures SR still occurs on a faster time-scales than the intrinsic fluorescence. Moreover, no change in the shape of the spectra is observed. At 150 K, the viscosity increase makes the formation of the states with a CT character difficult, and the fluorescence from the LE state prevails. Thus, a blue-shifted steady-state emission spectrum is observed. At 100 K, a polar glass is formed, which makes the solvent molecules immobile, preventing any change in the dye conformation, as well as solvent relaxation. Therefore, an emission spectrum, which is supposed to be in shape and energy comparable to that of a Franck Condon type, is observed (figure 4B). This spectrum is blue-shifted and the vibrational structure is visible. In order to find out to what extent solvent polarity influences the emission spectra in a glass system, we performed a temperature scan in a solvent with a significantly lower polarity (2-methyltetrahydrofurane). No significant difference in comparison to the spectra recorded in ethanol:methanol mixture was observed (data not shown here).

A different picture is observed for a nonpolar solvent such as heptane. The decrease in temperature does not lead to any important spectral shift. With decreasing temperature the contribution from the more energetic excited states starts to dominate over the lower-energy charge transfer state.

3.5 Time resolved emission spectra

The crucial point for quantitative SR studies presents the determination of "time 0 spectrum", i.e., the spectrum emitted prior to any change of the position and orientation of the solvent molecules ("Franck-Condon state"). The approximate procedure consists in subtracting the maximum of absorption spectrum measured in the investigated system from the difference between maxima of absorption and emission spectra measured in a reference non-polar solvent. For a precise description of this procedure

see a publication by Fee, et.al.[27] Unfortunately, this approach fails in case of the AS dyes. The above mentioned intramolecular process introduces an additional photophysical effect in the reference non-polar solvent. A wide range of molecules at various states contributes to the emission, which disables a simple determination of the steady state maximum of the non-relaxed state. Thus, an alternative method must be used in order to obtain a reasonable "time 0 estimate". As shown above (Table 1), the absorption and excitation spectra are rather independent of both the position of attachment of anthroyloxy group and of solvent used. Consequently, also the "time 0 spectrum" can be considered as to be almost invariant of those parameters.

It has been shown that the emission spectrum at the glassy state serves as a good approximation for "time 0 estimate" in a given solvent.[27] Moreover, the average frequency of those low temperature spectra appears to be rather independent of the choice of solvent and position of attachment of the anthroyloxy group (e.g., υ_{av} = 23 840 cm^{-1} and υ_{av} = 23 800 for 16-AP in EtOH+MetOH glass and 2-AS in 2-MTHF glass, respectively). Considering those arguments, we believe that the determined υ_{av} value of 23 800 cm^{-1} for 2-AS in 2-MTHF glass can be taken as a good estimate of the emission maximum of the Franck-Condon state of these AS-dyes in DMPC LUV. Taking into consideration that the maximum of the excitation and absorption spectra of those dyes in LUVs differs at the most by 200 cm^{-1} from the spectrum in heptane (Table 1) and that the absolute value of the determined Stokes-shifts in LUVs is about 2300 cm^{-1}, the maximal systematic error caused by the present "time 0 estimation" is lower than 10 %. Thus, a "time 0 value" of 23 800 cm^{-1} is considered as a valuable estimate and serves further as an input value for constructing the correlation functions *C(t)*.

As concluded above from the steady state emission data, a number of different states contribute to the photophysical behavior of n-AS dyes. Emission from different states take place in non-polar environments, however, the emission from the state with a CT character seems to dominate in polar systems. Naturally, solvent relaxation is present as well. These conclusions are also supported by the recorded time resolved emission spectra (TRES). A valuable parameter obtained by TRES is the time evolution of full width at half maximum (FWHM). The pure solvent relaxation process is characterized

by an increase at initial times followed by a decrease of FWHM.[3,17,28] Such a behavior is clearly observed for 2-AS (Figure 7). When more processes take place the time course of FWHM becomes more complex. This is the case for the curves measured for 9-AS and 16-AP. The steep decline at very early times (up to 1 ns) indicates that there occurs a fast process, which remains partially unresolved.

Another important parameter yielded by the TRES is an overall Stokes shift that characterizes the micropolarity of the dye microenvironment. This is also true for AS-dyes featuring quite complex photophysics. As evident from Table 4, the Stokes shift, which is proportional to micropolarity, decreases with deeper location of the chromophore. Interestingly, even though the 2-AS and 9-AS dyes are reported to be located close to each other (0.08-0.19 nm)[6] a large change in $\Delta\upsilon$ is observed. This fact supports the idea of a steep change in water density along the z-axes in the carbonyl region of the bilayer.[5,29] Moreover, the difference in $\Delta\upsilon$ between 9-AS and 16-AP is almost negligible although their mutual distance was estimated between 0.3 and 0.5 nm,[6] confirming the presence of the highly dehydrated backbone region.[5,29] However, comparison to the data measured in the paraffin oil, where the smallest $\Delta\upsilon$ was observed, evokes that some water molecules are still present even for 16-AP. A possible explanation is that the chromophore which naturally interacts with the dipoles of water noncovalently may draw the water molecules into the backbone region. Parallel trends are found for the preferential solvation in mixtures of two liquids.[30]

In the previous paragraph we concluded that with the deeper localization of the dye its microenvironment becomes less polar. This means that the dye microenvironment starts to be more and more similar to that present in the hydrocarbon-like systems (for instance hexane). However, maxima in the FWHM time profiles (Figure 7) are apparent for both 9-AS and 16-AP at longer times indicating that part of the relaxation process happens via solvent relaxation. This fact might again point to the presence of water molecules in the region near the center of the bilayer. In order to prove that the faster process indeed represents the internal intramolecular relaxation TRES were also scanned in paraffin oil that has a slightly higher viscosity (reported values obtained by diphenylhexatriene anisotropy studies: 1.9 P for paraffin oil[31] and 0.8-1.4 P for the center of bilayer in the liquid crystalline phase at given

temperature).[32] The obtained FWHM time profile exhibits a steep early decline as in the case of 16-AP in DMPC LUV, while at longer times the FWHM dependence remains almost constant. This fact suggests that intramolecular dynamics occurs on a faster timescale than the diffusion part of the solvent relaxation process.

From the visual inspection of the correlation functions (Figure 8), which provides the information on the kinetics of the relaxation process, it is evident that with the deeper location of the dye the dynamics of relaxation becomes faster on the whole. However, multiexponentional fitting (Table 4) reveals that more processes contribute. In case of 2-AS, two exponentials of the order of nanoseconds are sufficient to provide a satisfactory fit, with more than 90% of relaxation process being captured. Such a behavior was found to be typical for dyes that undergo the relaxation process mostly via solvent relaxation and are located at the headgroup region.[3,33,34] Moreover, the integral relaxation time is in the range of 2 ns implying that 2-AS occupies a similar region and features a similar solvation behavior as the already reported headgroup probes, for instance Patman.[3] When investigating 9-AS and 16-AP, at least three exponentials are needed for a reasonable fitting. The fastest component (<50 ps) that is likely to be assigned to the dye photophysics becomes more significant upon moving towards the center of the bilayer. In contrast, the slowest components, that are believed to correspond to the solvent relaxation, become less significant, and their time values grow larger moving towards the deeper interior of the bilayer. The integral relaxation times characterizing the overall relaxation process become smaller with a deeper location of the dye, which is also apparent from the visual inspection of the correlation functions. The data measured in paraffin oil yield similar results to those found for 16-AP in DMPC LUVs. The observed slower integral relaxation time and the nanosecond component of the fit can be ascribed to the larger viscosity of the paraffin oil.

3.6 Dynamics of the n-AS solvation and intramolecular relaxation

The experimental data indicate that the relaxation process of AS-dyes in phospholipid bilayers is rather complex. The time resolved emission spectra reflect both intramolecular and intermolecular

dynamics. The intramolecular relaxation includes torsional relaxation, formation of a charge transfer state, and also other rearrangements of the carboxylic moiety leading to non-polar emitting states. At the same time, solvent relaxation takes place. These two processes can not be completely separated from each other. The rate of the LE→ CT transition will most certainly depend on the polarity of the dye microenvironment. The time scale for the faster components of the solvent relaxation (libration, rearrangement, etc.) is roughly comparable with the intramolecular relaxation. We believe, however, that the intramolecular relaxation occurs on a subnanosecond timescale. This is supported by results of ab initio calculations. The intersection between the locally excited state and the charge transfer state occurs only 0.2 eV above the locally excited minimum. The transition state leading to the CT state is thus energetically well accessible and the rate of this transition is only limited by intramolecular energy transfer between modes. The same holds true for the transition to the other emitting states.

We can conclude that the slowest process observed in the time resolved fluorescence spectra corresponds to the diffusion part of solvent relaxation. The use of n-AS dyes is, therefore, justified for solvation studies of phospholipids bilayers where the diffusion driven solvent relaxation plays a dominant role. From the results of the time-resolved experiments the following conclusions about the solvation dynamics in the lipid bilayers can be drawn. First, as we go deeper into the bilayer the solvation contribution to the response functions becomes less significant but does not disappear completely even for the most buried 16-AP. This clearly indicates that some water is present even in the very hydrophobic parts of the bilayer. Second, the diffusion solvent relaxation becomes slower upon approaching the center of the bilayer. What we observe is essentially preferential solvation in a mixture of a polar and non-polar solvents. While the non-polar solvent (in our case fatty acid chains) does not contribute significantly to the Stokes shift, the polar molecules (water in our case) contributes more or less proportionally to the number of surrounding solvent molecules. With decreasing water concentration we observe a decreasing Stokes shift and the solvation times get longer.[35] If we considered the diffusion constant to be independent of the distance from the bilayer head, we should be in principle able to reconstruct the water concentration profile. Unfortunately, our data at this point are

too noisy for such a reconstruction. The obtained data, however, qualitatively support the results of molecular dynamical simulations. These are showing a steep decrease of water concentration from the headgroup to the backbone region of the bilayer.[36] Certain amount of water is, however, always present even in the backbone region. Note also that the headgroup region of the bilayer is coarse and the water profile reflects mostly the roughness of the surface. It would be, therefore, desirable to investigate the precise location of the n-AS dye in the bilayer, which will be the subject of a subsequent study.

4. Conclusions

We have explored the nature of light emitting states of n-AS dyes by combining fluorescence spectroscopy with quantum chemical calculations. The recorded time resolved emission spectra revealed a non-trivial behavior of these dyes in the backbone region of the phospholipid bilayer, showing the presence of multiple relaxation processes. Thus, steady state fluorescence spectra were recorded in systems of varying viscosity and polarity to elucidate the n-AS photophysics. In addition, quantum chemical calculations have been performed for a model 9-methylanthroate dye. Combining these two approaches, we have shown that the mere relaxation to the locally excited state after the primary excitation cannot account for the experimentally observed behavior. Existence of an emitting state of a charge transfer character was, therefore, suggested and confirmed by means of high level *ab initio* calculations. We have also estimated the barrier between the locally excited state and the other emitting states. Time resolved experiments have been discussed focusing on these new photophysical findings. We have concluded that time resolved fluorescence measurements using the n-AS dye can serve as a valuable source of information on the diffusion-controlled part of solvent relaxation, while processes on femtosecond and picosecond timescales reflect in a rather complex way also intramolecular relaxation of the chromophore.

ACKNOWLEDGEMENT

We thank the Grant Agency of the Academy of Sciences of the Czech Republic for support via a grant A400400503. This work has been also supported by the Czech Ministry of Education (grants LC512 and LC06063).

REFERENCES

(1) Milhaud, J. *BBA-Biomembranes* **2004**, *1663*, 19.

(2) Bursing, H.; Ouw, D.; Kundu, S.;Vohringer, P. *Phys. Chem. Chem. Phys.* **2001**, *3*, 2378.

(3) Sýkora, J.; Kapusta, P.; Fidler, V.; Hof, M. *Langmuir* **2002**, *18*, 571.

(4) Forrest, L.R.; Sansom, M.S.P. *Curr. Opin. Struct. Biol.* **2000**, *10*, 174.

(5) Zubrzycki, I.Z.; Xu, Y.; Madrid, M.;Tang, P. *J. Chem. Phys.* **2000**, *112*, 3437.

(6) Abrams, F.S.; Chattopadhyay, A.; London, E. *Biochemistry* **1992**, *31*, 5322.

(7) Villalain, J.; Prieto, M. *Chem. Phys. Lipids* **1991**, *59*, 9.

(8) Werner, T.C.; Hoffman, R.M. *J. Phys. Chem.* **1973**, *77*, 1611.

(9) Berberan-Santos, M.N.; Prieto, M.J.E.; Szabo, A.G.; *J. Phys. Chem.* **1991**, *95*, 5471.

(10) Hutterer, R.; Schneider, F.W.; Lanig, H.; Hof, M. *BBA-Biomembr.* **1997**, *1323*, 195.

(11) Chattopadhyay, A.; Mukherjee S. *Langmuir* **1999**, *15*, 2142.

(12) Maroncelli, M. *J. Mol. Liq.* **1994**, *57*, 1.

(13) Michael, D.; Benjamin, I. *J. Chem. Phys.* **2001**, *114*, 2817.

(14) Cichos, F.; Brown, R.; Rempel, U.; von Borczyskowski, C. *J. Phys. Chem. A* **1999**, 26506.

(15) Tamashiro, A.; Rodriguez, J.; Laria, D. *J. Phys. Chem. A* **2002**, *106*, 215.

(16) Hope, M.J.; Bally, M.B.; Mayer, L.D.; Janoff, A.S.; Cullis, P.R. *Chem. Phys. Lipids* **1986**, *40*, 89.

(17) Horng, M.L.; Gardecki, J.A.; Papazyan, A.; Maroncelli, M. *J. Phys. Chem.* **1995**, *99*, 17311.

(18) Granucci, G.; Toniolo, A. *Chem. Phys. Lett.* **2000**, *325*, 79.

(19) Molpro 2002.6 , Werner, H.J.; Knowles, P.

(20) Mopac 2000, Stewart, J. J. P., Fujitsu Limited, Tokyo, Japan (1999).

(21) Turro, N.J. *Modern Molecular Photochemistry*, University Science Books, Sausalito: 1991.

(22) Werner, T.C.; Hercules, D.M. *J. Phys. Chem.* **1969**, *73*, 2005.

(23) Werner, T.C.; Matthews, T.; Soller, B. *J. Phys. Chem* **1976**, *80*, 533.

(24) Swayambunathan, V.; Lim, E.C. *J. Phys. Chem.* **1987**, *91*, 6359.

(25) Matayoshi, E.D.; Kleinfeld, A.M. *Biophys. J.* **1981**, *35*, 215.

(26) Dey, J.; Haynes, J.L.; Warner, I.M.; Chandra, A.K. *J. Phys. Chem.* **1997**, *101*, 2271.

(27) Fee, R.S.; Maroncelli, M. *Chem. Phys.* **1994**, *183*, 235.

(28) Richert, R. *J. Chem. Phys.* **2001**, *114*, 7471.

(29) Nagle, J.F.; Tristram-Nagle, S. *BBA-Reviews on Biomembr.* **2000**, *1469*, 159.

(30) Petrov, N.K. *High Energy Chem.* **2006**, *40*, 22.

(31) Mateo, C. R.; Lillo M. P.; Brochon, J. C.; Martlnez-Ripoll, M.; Sanz-Aparicio, J.; Acuiia A.U. *J. Phys. Chem.* **1993**, *97*, 3486.

(32) Lopez Cascales, J.J.; Huertas, M.L.; de la Torre J.G. *Biophys. Chem.* **1997**, *69*, 1.

(33) Dutta, P.; Sen, P.; Mukherjee, S.; Bhattacharyya, K. *Chem. Phys. Lett.*, **2003,** *382*, 426.

(34) Halder, A.; Sen, S.; Das Burman, A.; Patra, A.; Bhattacharyya, K. *J. Phys. Chem. B* **2004**, *108*, 2309.

(35) Agmon, N. *J. Phys. Chem. A* **2002**, *106*, 7256.

(36) Jadlovszky, P.; Mezei, M. *J. Chem. Phys.*, **1999**, *111*, 10770.

Table 1: Maxima of excitation spectra in 2-AS in various systems. The three rows correspond to the three main peaks as described in the text:

Solvent	υ_1 (cm^{-1})	υ_2 (cm^{-1})	υ_3 (cm^{-1})
Heptane	26 340	27 700	29 150
Paraffin oil	26 150	27 550	28 900
Propanol	26 200	27 600	28 970
Ethanol + methanol	26 240	27 700	29 000
DPPC LUV (25 ^{o}C)	26 100	27 470	28 910
DPPC LUV (46 ^{o}C)	26 100	27 490	28 960
DMPC LUV	26 100	27 500	28 990

Table 2: Maxima of excitation spectra of "AS-dyes" in various systems (the middle peak (υ_2) of excitation spectrum is taken into account):

Solvent	2-AS υ_2 (cm^{-1})	9-AS υ_2 (cm^{-1})	16-AP υ_2 (cm^{-1})
Heptane	27 700	27 700	27 760
Paraffin oil	27 550	27 550	27 550
Propanol	27 600	27 620	27600
Ethanol + methanol	27 700	27 700	27680
DMPC LUV	27 500	27 480	27 550

Table 3. Characterization of important minima on the S_1 potential energy surface of the 9MA molecule. FC denotes the Franck-Condon point, LE is a locally excited state, Min1-3 are other local minima. Energies at the CAS-SCF(6/6) and corresponding CASPT2 levels are displayed in electronvolts, relative to the FC point.

	FC	LE	Min1	Min2	Min3
CAS/eV	0	-0.6	-0.45	-0.8	-0.7
S_0/S_1 gap/eV	4.7	4.25	3.3	1.9	1.8
CASPT2/eV	0	0.05	-0.2	0.4	0.85
S_0/S_1 gap/eV	4.2	3.91	2.6	1.9	2.5
GS dipole/Debye	1.9	2.0	2.1	3.3	2.1
ES dipole/Debye	2.3	1.9	6.5	2.1	1.1
Transition dipole /Debye	0.38	0.65	3.4	0.12	0.27

Table 4: Characteristics obtained by analyzing correlation functions in DMPC LUVs and in paraffin oil. ν_{t0} corresponds to the spectral maximum of "time 0 estimate", $\Delta\nu$ is the overall Stokes shift, τ_i and a_i are the times and amplitudes gained by a three-exponential fitting of the autocorrelation curve with equation [2].

	ν_{t0} (cm^{-1})	$\Delta\nu$ (cm^{-1})	τ_1 [ns] † (a_1)	τ_2 [ns]† (a_2)	τ_3 [ns] † (a_3)	τ_r [ns]	%SR obsd
2 AS	23800	2350	0.91 (0.38)	3.23 (0.62)	- -	2.31	93
9 AS	23800	1900	<0.05 (0.46)	0.69 (0.19)	4.32 (0.35)	1.70	74
16 AP	23800	1850	<0.05 (0.73)	0.51 (0.22)	6.00 (0.04)	0.23	26
2 AS	23800	1630	<0.05 (0.50)	0.39 (0.21)	1.56 (0.29)	0.58	44

†) We are aware of the fact that the interpretation of 3-exponential fitting is rather speculative, especially when the amplitudes do not reach high values.

FIGURE CAPTIONS

Figure 1. A. Schematic structures of DMPC, 2-AS, 9-AS, and 16-AP. Approximate localization of the n-AS dyes relative to the lipid molecules are depicted ~~sighned~~. B. Structure of 9-methylanhroate (9MA).

Figure 2. Emission spectra of AS dyes in heptane (A) and paraffin oil (B), solid line: 2-AS, dotted line: 9-AS, dash-dotted line: 16-AP.

Figure 3. Emission spectra of AS dyes in ethanol-methanol mixture (1:1) (A) and DMPC LUV (B), solid line: 2-AS, dotted line: 9-AS, dash-dotted line: 16-AP.

Figure 4. Temperature scan of emission spectra of AS dyes in heptane (the spectra were recorded at 300 K, 280 K, 260 K, 240 K, 220 K, 200 K, 190 K and the intensity increases with decreasing temperature monotonously) (A) and in ethanol-methanol mixture (1:1) (B).

Figure 5. Relaxed torsional potential for S_0 and S_1 states of 9-methylanthroate calculated at AM1-FOMO-6/6 level. Full line corresponds to the S_0 state, while the dashed line to the S_1 state. The S_1 potential has been shifted by -3.2 eV.

Figure 6. Important structures on the S_1 state of 9-methylanthroate. The Franck-Condon geometry has been obtained as a ground state minimum using MP2/6-31g* method, all the excited states minima and the S2/S1 conical intersection have been obtained by CAS-SCF 6/6 method using the same basis.

Figure 7. FWHM time profiles of AS-dyes in DMPC LUV (empty symbols) and paraffin oil (solid symbols), squares: 2-AS, triangles: 9-AS, stars: 16AP, circles: 2-AS in paraffin oil.

Figure 8. Correlation functions of AS-dyes in DMPC LUV (empty symbols) and paraffin oil (solid symbols), squares: 2-AS, triangles: 9-AS, stars: 16AP, circles: 2-AS in paraffin oil.

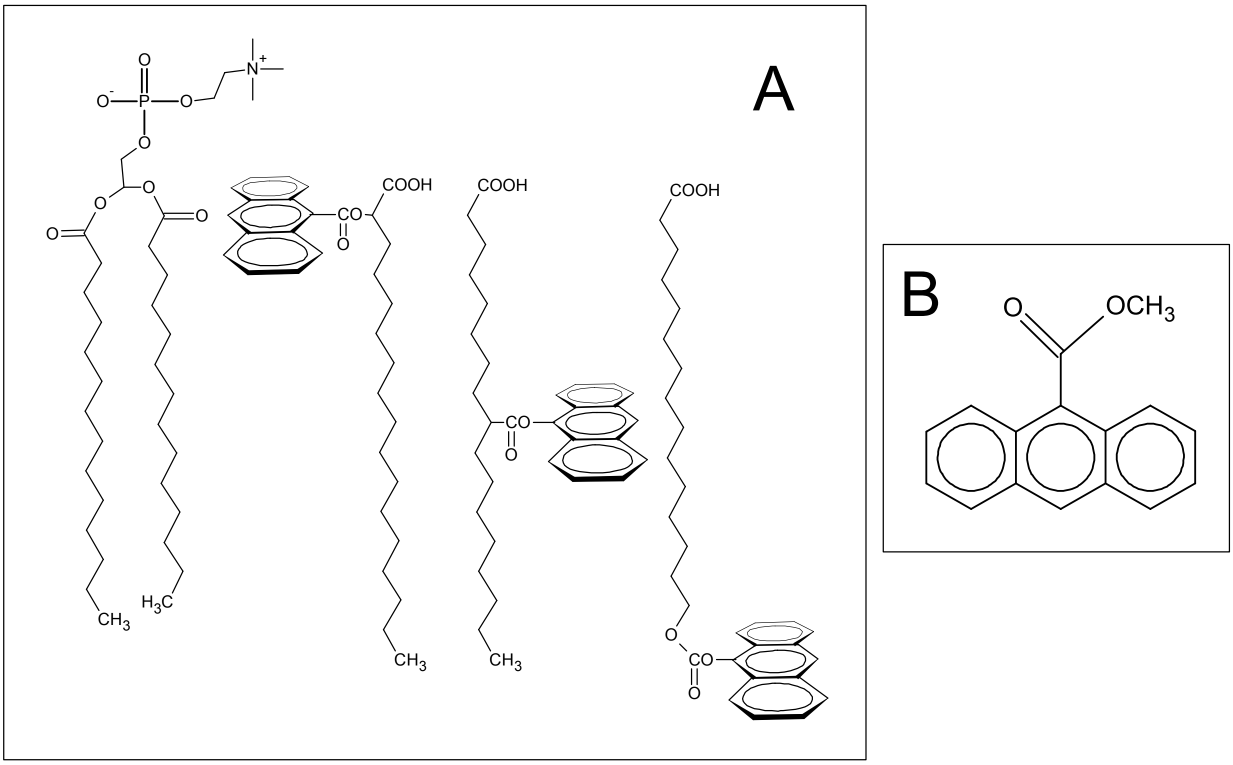

Figure 1.

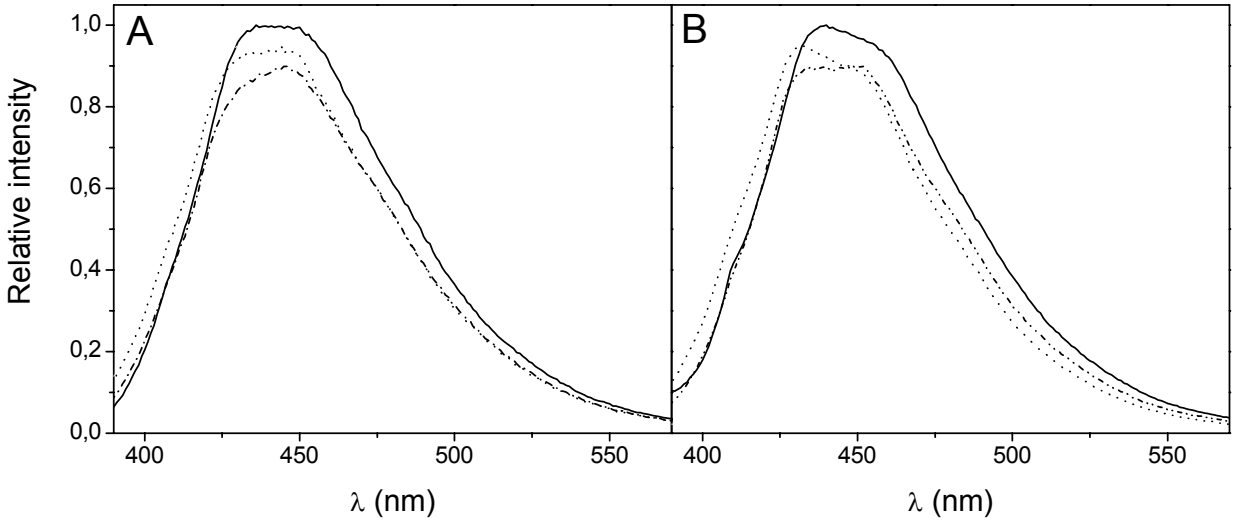

Figure 2.

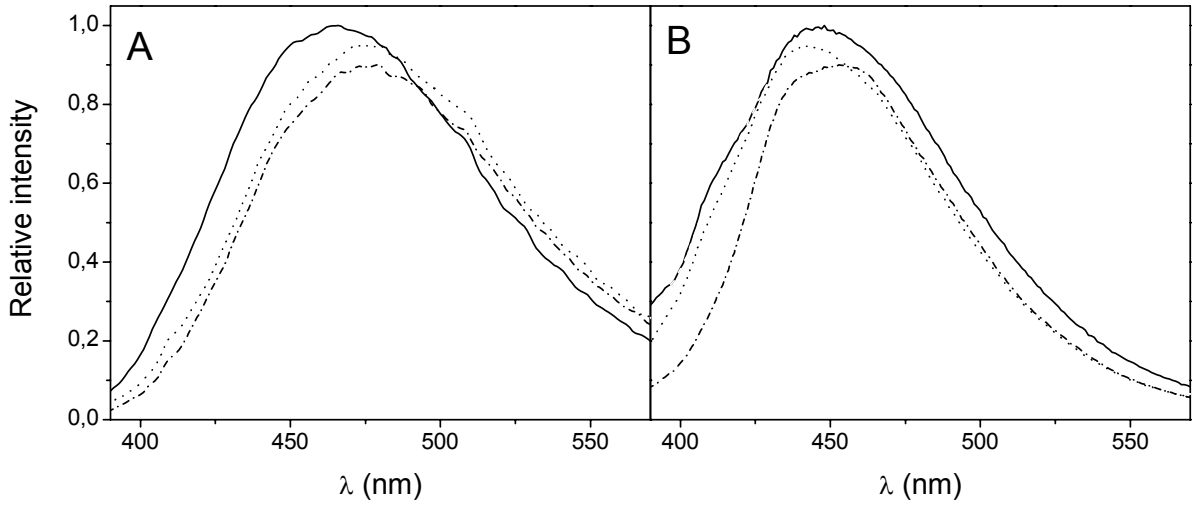

Figure3.

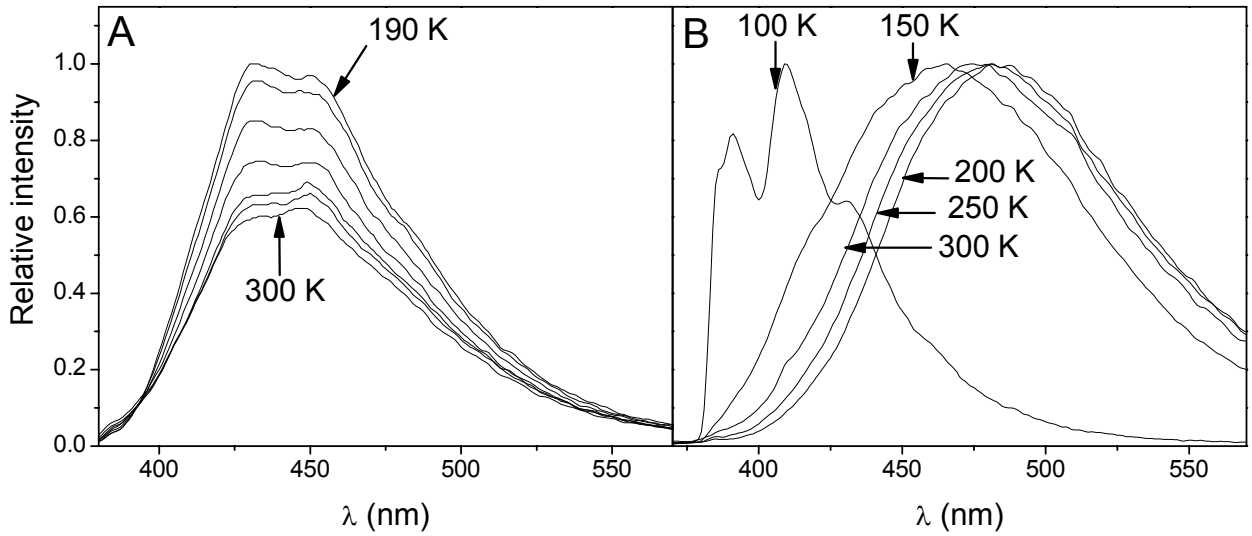
A
190 K
300 K
Relative intensity
1.0
0.8
0.6
0.4
0.2
0.0
400
450
500
550
λ (nm)
B
100 K
150 K
200 K
250 K
300 K
400
450
500
550
λ (nm)

Figure 4.

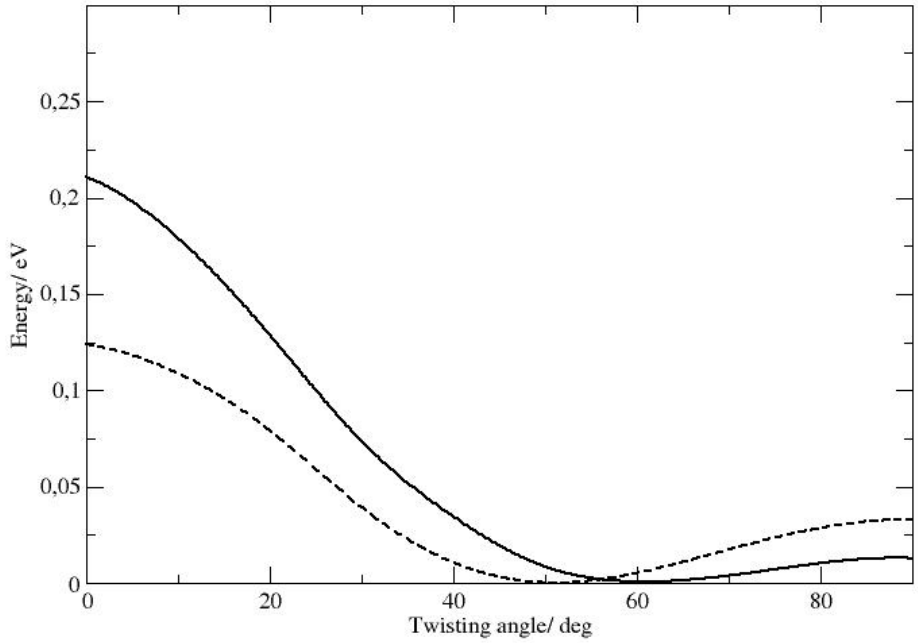

Figure 5.

Franck-Condon geometry

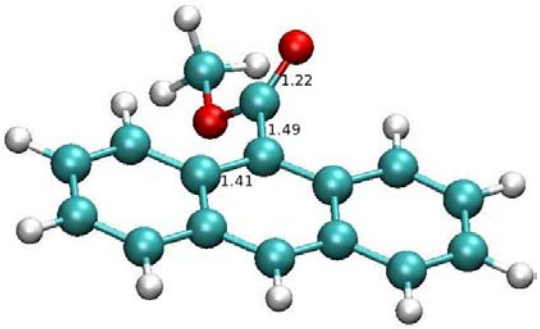

Locally excited state

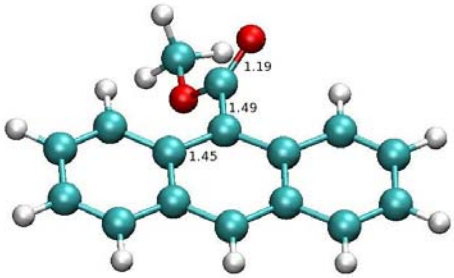

Min1

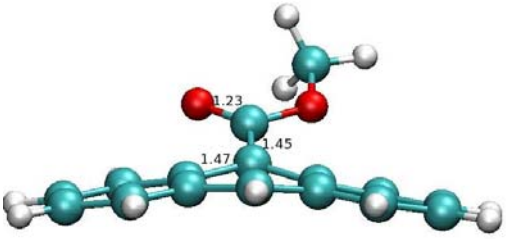

S_2/S_1 conical intersection

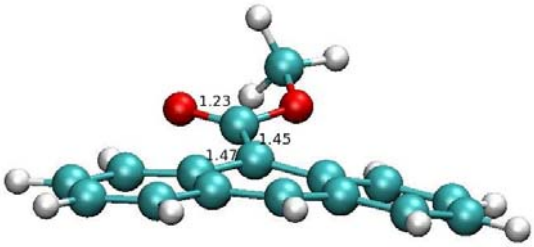

Min2

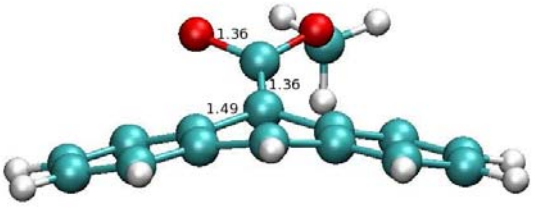

Min3

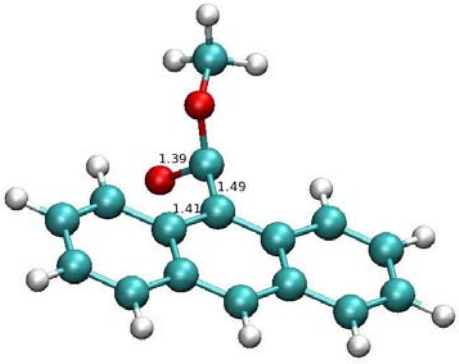

Figure 6.

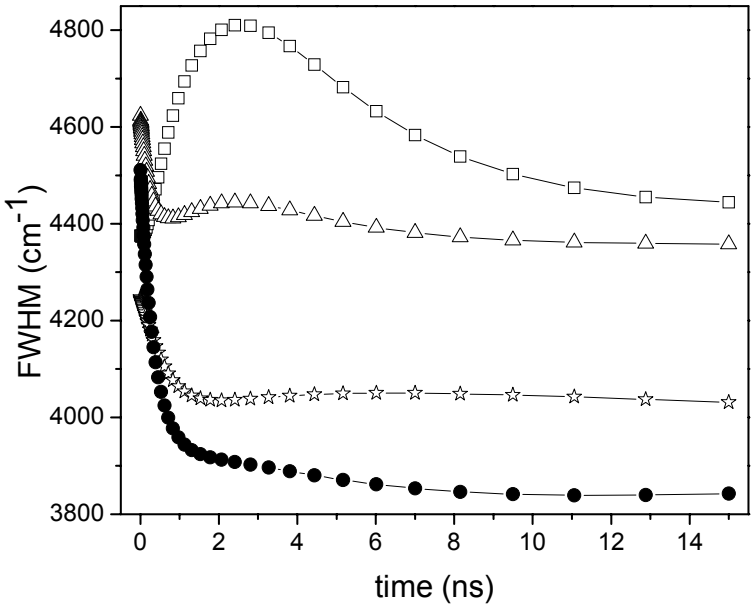

Figure 7.

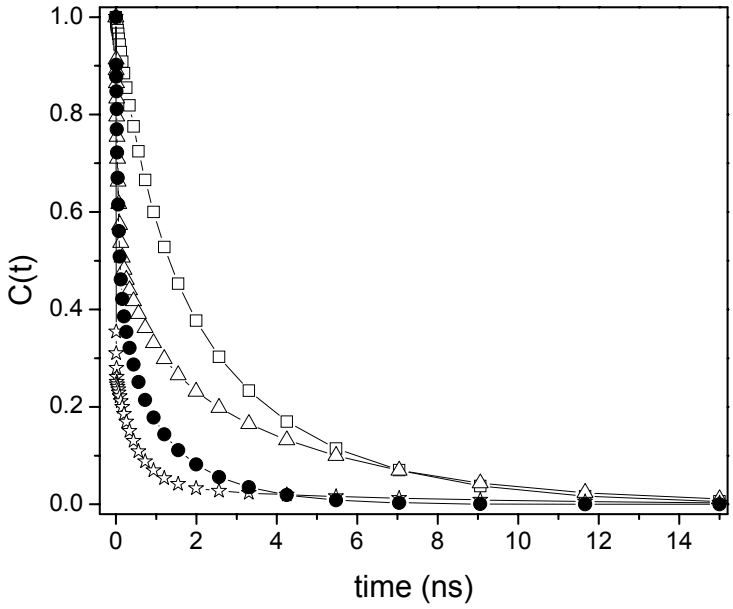

Figure 8.